ENERGETIKA. 2012. T. 58. Nr. 3. P. 166–172

Gas sensitivity of stoichiometric and excess-iron Ni-Zn ferrite prepared by sol-gel auto-combustion

Andris Sutka,

Gundars Mezinskis,

Gundars Strikis,

Andreis Siskin

Institute of Silicate Materials,
Riga Technical University,
Azenes 14/24, LV-1048, Riga, Latvia
E-mail: andris.sutka@rtu.lv

Application of new materials offers more sensitive, selective and long-term stable sensor materials. The aim of the present work is to compare gas response to acetone of nanostructured sol-gel auto-combustion derived stoichiometric and excess-iron cubic spinel type nickel-zinc ferrite ($Ni_{0.3}Zn_{0.7}Fe_{2+z}O_4$ where z = 0 and 0.1). Detailed synthesis steps and gas sensing measurement methodology were described. The sensor material was characterized by x-ray diffraction (XRD), scanning electron microscopy (SEM) and direct current (DC) resistance measurements. XRD analysis confirms that samples form the single-phased cubic spinel structure, SEM reveals nanosized grains less than 100 nm in diameter. Plots of resistance versus temperature show adsorbed water contribution to the conductance. With excess-iron, Ni-Zn ferrite changes its DC electrical resistivity, type of conductivity, as well as response to reducing gas (more than 2 times). Obtained relationships can be explained with Fe^{2+} formation in the material, thus increasing charge carrier (electron) concentration. This leads down to higher oxygen adsorption ability which can act with test gas.

Key words: nickel-zinc ferrite, non-stoichiometry, gas sensor, combustion synthesis

INTRODUCTION

Spinel ferrites are important technological materials due to their semiconducting and ferrimagnetic properties [1]. Recently, ferrites due to their semiconducting behaviour have been used as gas sensitive materials. A large number of stoichiometric spinel ferrites, for example, $ZnFe_2O_4$, $NiFe_2O_4$, $CdFe_2O_4$, $MgFe_2O_4$, $CuFe_2O_4$, $CoFe_2O_4$, $NiZnFe_2O_4$, $MnZnFe_2O_4$, $MgZnFe_2O_4$, etc., have shown sensitivity to certain gases [2–7]. At the same time information about ferrite gas sensors in comparison with single metal oxide gas sensors is still limited and does not contain data about gas sensing properties of complex or non-stoichiometric iron deficient or excess-iron spinel ferrite compounds, which have essentially different electrical properties.

The conductivity in spinel ferrites is due to hopping of charge carriers (electrons or holes) between cations presented by more than one valence state occupying the octahedral sites [8]. Zinc or cadmium ions show strong affinity to the tetrahedral site, but iron, nickel, manganese, and cobalt ions, for example, show tendency to occupy octahedral sites. Electron hopping between Fe^{3+} and Fe^{2+} provides n-type, but hole hopping between $Ni^{3+} \leftrightarrow Ni^{2+}$, $Mn^{3+} \leftrightarrow Mn^{2+}$, $Co^{3+} \leftrightarrow Co^{2+}$ provides p-type conductivity.

The gas sensitivity of metal oxide semiconductor sensors is highly affected by their electric and transport properties [9]. In our previous works, influence of zinc ion concentration on resistance and sensitivity of p-type nickel ferrite [10], as well as iron ion non-stoichiometry effect on resistance and sensitivity of n-type zinc ferrite [11] were investigated. It was found that with zinc addition to nickel ferrite, response to different VOCs decreases, attributed to extinguishing p-type charge carriers (holes) and carrying a small amount of dopants in the semiconductor structure. This was confirmed with change of conductivity type by increasing temperature. In case of zinc ferrite response increased by going from iron deficiency to excess due to an increase of Fe^{2+} concentration, the charge carrier (electron) concentration increased, leading down to increase adsorbed oxygen species on grain surface. It is known that n-type materials surface coverage with oxygen ions at elevated temperature is limited by the supply of electrons. Higher charge carrier concentration leads to increase of adsorbed oxygen species on the surface, thus larger change of the resistance due to interaction with reactive gas could be expected [12].

The aim of the present work is to compare gas sensitivity of stoichiometric and excess-iron $Ni_{0.3}Zn_{0.7}Fe_{2-z}O_4$. It is interesting if iron-excess Ni-Zn ferrite will show higher response towards volatile organic compounds (VOCs) in comparison with stoichiometric Ni-Zn ferrite, as it was observed for $ZnFe_2O_4$ in our previous work because Ni ion restricts, but excess-iron enhances Fe^{2+} formation, thus increasing charge carrier (electron) concentration in the Ni-Zn ferrite material.

METHODOLOGY

Synthesis and sample preparation

The ferrite samples with the chemical formula $Ni_{0.3}Zn_{0.7}Fe_{2+z}O_4$ ($z = 0$ and 0.1) were prepared by using sol-gel auto-combustion [13]. Analytical grade desired metal nitrates according to the molar proportions were dissolved in distilled water. Then 1 mole of citric acid monohydrate ($C_6H_8O_7 \cdot H_2O$) was added to the solution. Metal nitrates act as an oxidizing agent, but carboxylate groups in citric acid act as a reducing agent for combustion reaction. To increase metal cation chelating with citrates, nitrate / citric acid mixture was neutralized (pH = 7) by using ammonium hydroxide (NH_4OH) 26% solution in water. The obtained solution was mixed in a 100 cm^3 chamotte crucible and evaporated at 80 °C temperature under stirring until viscous gel was formed. Additionally, the gel was dried for 24 hours to remove water residues and obtain xerogel. Gel was heated up to 250 °C to initiate combustion reaction, and the ferrite powder was obtained. The synthesis steps of the ferrite samples are shown in Fig. 1.

Ferrite samples in the pellet form for D. C. resistance and gas sensing measurements with 10 mm diameter and 1 mm thickness were prepared from as-burnt ferrite powders in a uniaxial press by keeping the sample under 5 MPa for 3 minutes. After sample formation sintering at 800 °C for 1 hour was performed. As a binder, 10 l solution of polyvinyl-alcohol with a concentration 10 wt% was used.

Characterization

For crystalline structure analysis the XRD analysis was used. XRD was recorded for 2θ from 10° to 60° at a scan rate of 1° min^{-1} using an Ultima + X-ray diffractometer (Rigaku, Japan) with CuKα radiation. Sample crystallite size was calculated by using the Debye-Scherrer equation Eq. (1):

$$D = \frac{k\lambda}{B \cdot \cos\theta}, \quad (1)$$

where D is the crystallite size (nm), k is the Scherrer constant (for cubic crystalline structures as spinels and spherical particles k is equal to 0.94), λ is the wavelength of the X-Ray radiation (0.154178 nm), B is the width at half maximum intensity in radians.

Microstructural studies were carried out with a Quanta 200 scanning electron microscope (FEI, Netherlands). For grain size and microstructure determination SEM was performed on fracture surfaces of sintered pellets.

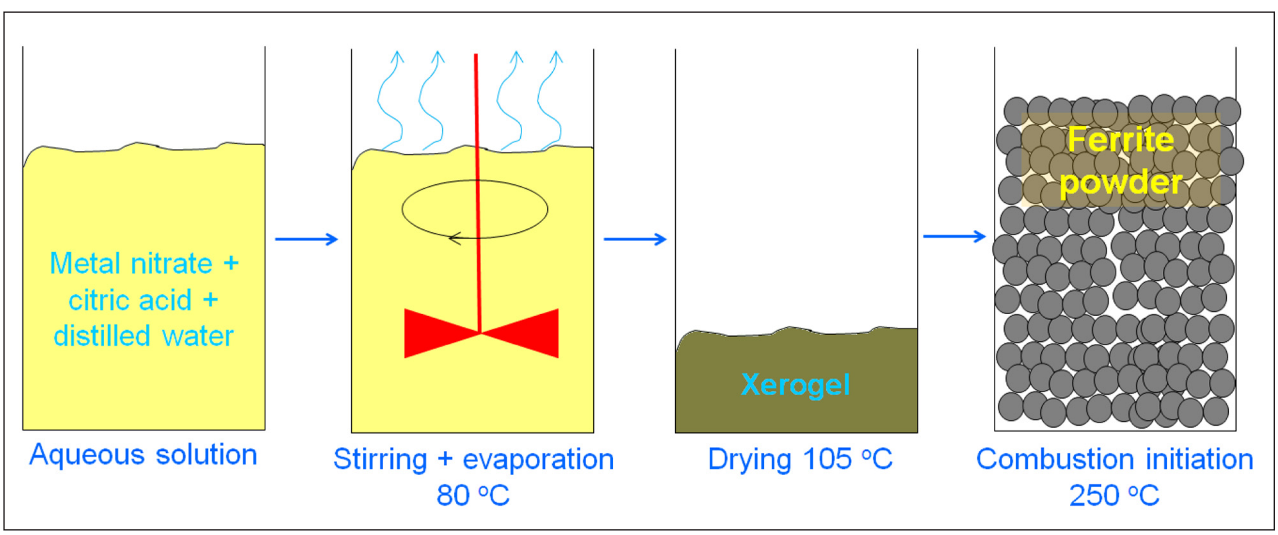

Fig. 1. Processing steps of ferrite nano-powders

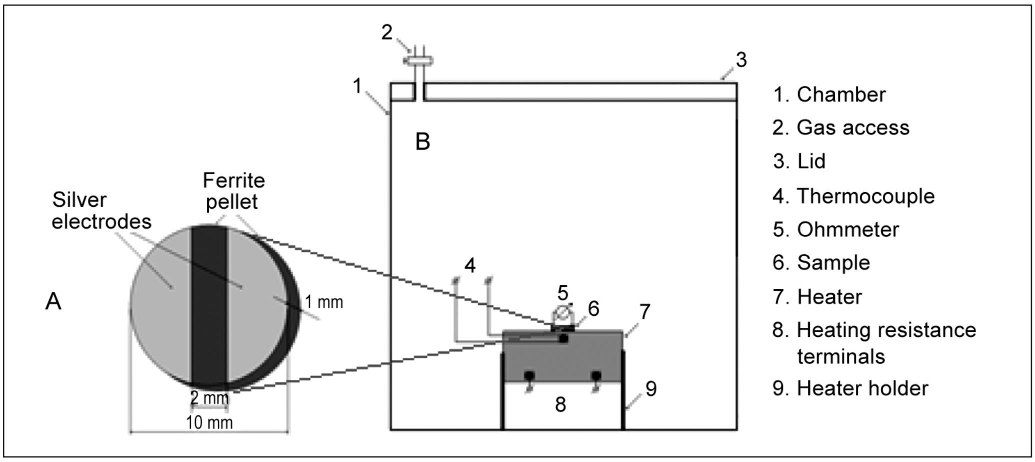

Fig. 2. Gas sensor element (A) and schematic representation of experimental array (B)

The DC electrical resistance was measured using the two probe constant current method. For temperature variation of electrical resistivity, the sample was kept in the closed chamber and maintained from 20 to 400 °C. Samples for electrical measurements from both sides were coated with high purity silver paint.

For sensing measurements the disks about 1 mm thickness and 10 mm in diameter were silvered on a face, as shown in Fig. 2A.

In order to improve their stability, the sensing elements before testing were heated at the desired temperature as recommended by other authors [14]. Then the sensor element was introduced in the Teflon chamber and placed on the chamotte heater. Since the sensitivity of gas sensors is greatly influenced by the operating temperature, the sensor was used to detect acetone vapours at various temperatures between 200 °C to 325 °C at ambient atmosphere pressure. At temperatures below 150 °C, the sensor surface is believed to be coverage with inactive –OH groups [15]. The test gas was injected into the chamber with a micropipette through the inlet.

Required gas concentration was calculated using Eq. (2):

$$V = \frac{C_{ppm} V_a M}{24.5 \times 10^9 D}, \qquad (2)$$

where V is the required liquid volume (cm^3), D is the density of the liquid (g/cm^3), V_a is the volume of the test chamber (cm^3), M is the molecular weight of the liquid (g/mol) [16].

The response S was determined with Eq. (3):

$$\begin{cases} S = \dfrac{R_a}{R_g} & \text{if} \quad R_g < R_a \\ S = \dfrac{R_g}{R_a} & \text{if} \quad R_g > R_a \end{cases}, \qquad (3)$$

where R_a is the clean air resistance but R_g is the resistance in the presence of test gas at the given temperature [2].

Overall, the chematic representation of experimental arrangement is shown in Fig. 2B.

RESULTS AND DISCUSSIONS

Characteristics of sensor material

The diffraction pattern of the ferrite samples after sintering at 800 °C is shown in Fig. 3. Sintering forms the pure cubic spinel type structure and no additional peaks are observed ensuring the phase purity. Crystallite size (Table) for material was calculated by means of line broadening of the most intense (311) diffraction peak and is located about 35 deg for both compositions. The pore fraction calculated by considering the experimental density and the theoretical density (observed from X-Ray data) of the sintered pellets were above 60%, thus satisfying requirements for materials used as gas sensors [17].

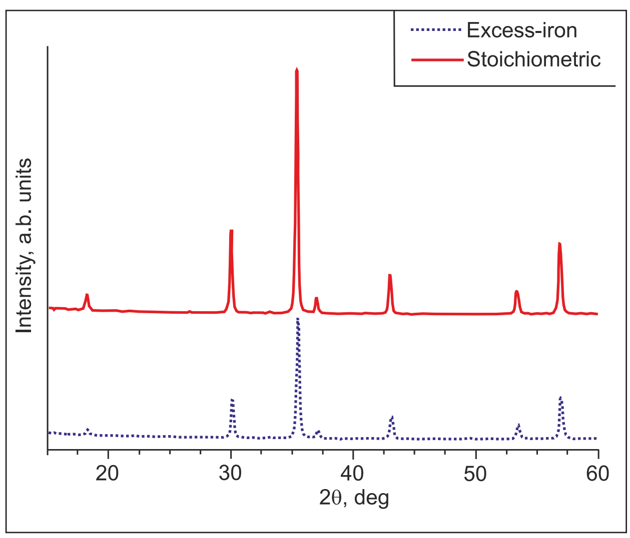

Fig. 3. XRD pattern of Ni-Zn ferrite samples sintered at 800 °C. All unmarked peaks correspond to spinel lattice different reflecting planes. Other peaks for impurity phases were not detected

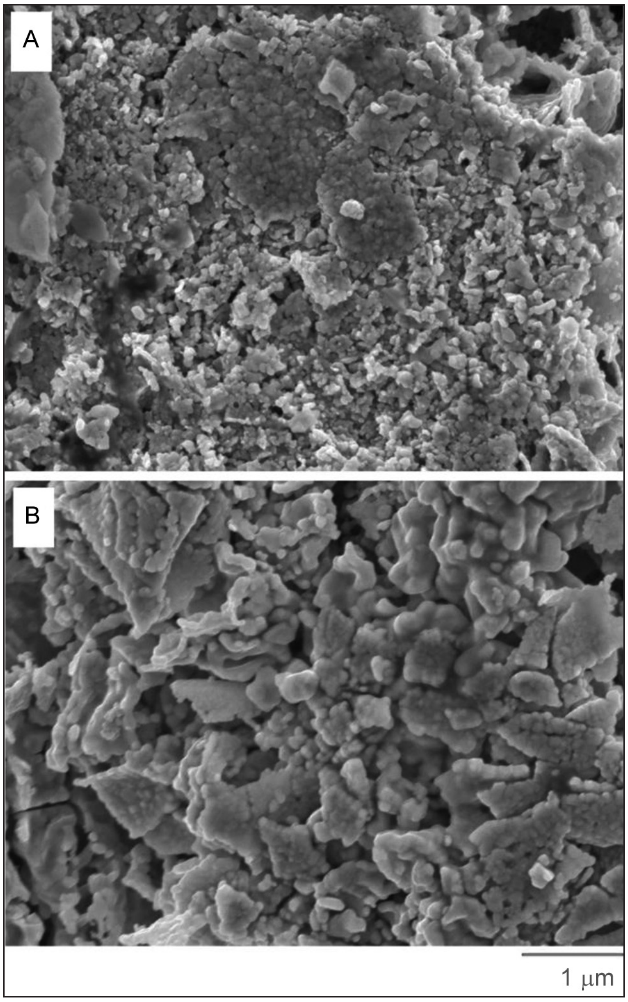

Fig. 4. SEM micrographs of stoichiometric (A) and iron-excess (B) Ni-Zn ferrite gas sensor sample fractured surfaces

Fig. 4. shows the typical SEM image of the sintered ferrite sample fractured surfaces. It can be seen that the microstructure of the samples consists of nanosized grains. The presented structure is suitable for gas sensing applications because nanosized grains possess high specific surface area for gas / solid interaction thus increasing response to analytical gases [18]. Generally, no morphological differences were apparent between samples with differing iron content.

Resistance and its dependence from temperature

Room temperature DC electrical resistivity for stoichiometric and excess-iron samples was $3.9 \cdot 10^8$ and $1.4 \cdot 10^7\ \Omega \cdot$ m, respectively. Decrease of the resistance for excess-iron

Table. **Some properties of gas sensor elements**

Parameter	Value
Crystallite size, nm	35 ± 2
Grain size, nm	<100
Porosity, %	65 ± 2

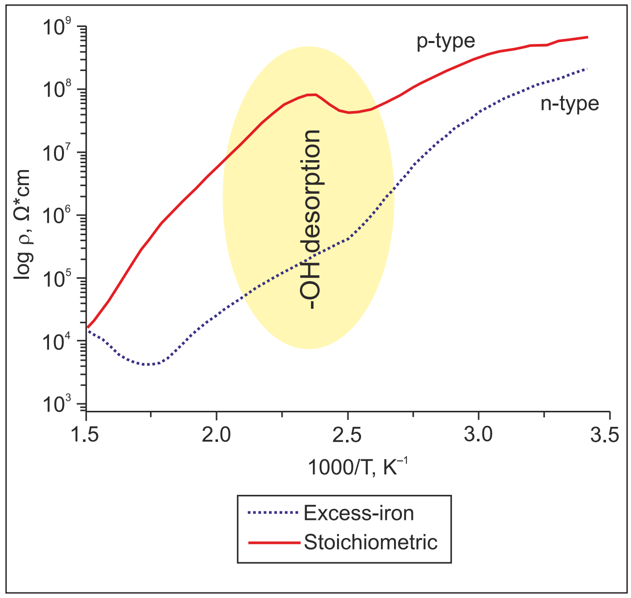

Fig. 5. D. C. resistivity as a function of temperature for stoichiometric and excess-iron ferrite samples

Ni-Zn ferrites in comparison with stoichiometric Ni-Zn ferrites is attributed to an increase of Fe^{2+} concentration, thus increasing the electron concentration [18].

The resistivity dependence on temperature is shown in Fig. 5. The resistance decreases by increasing the operating temperature showing the semiconductor behaviour. In the same time, the plot log ρ versus the operating temperature produces an anomalous change of resistance. Increase (for p-type) or decrease (for n-type) of the resistance is attributed to desorption of chemisorbed water [19]. Adsorption of water traps e^- from metal oxide semiconductor conduction or valence band in case of n-type or p-type semiconductor according to the equation $H_2O + e^- \leftrightarrow OH^-$ [20]. Desorption at higher temperatures returns $e^-$and hence increases (p-type) or decreases (n-type) resistance of the material $OH^- - e^- \leftrightarrow H_2O$ [20]. Desorption of chemisorbed water will promote oxygen adsorption and enhance sensitivity [21].

Gas sensing properties

The gas sensing response to acetone for stoichiometric and excess-iron Ni-Zn ferrites at concentration 500 ppm as a function of operating is shown in Fig. 6. Excess-iron Ni-Zn ferrite ($Ni_{0.3}Zn_{0.7}Fe_{2.1}O_{4-}$) exhibits higher response at all tested temperatures. The observed relationship is attributed to high Fe^{2+} concentration in the non-stoichimetric Ni-Zn ferrite, thus increasing the charge carrier (electron) concentration and leading to higher oxygen adsorption in turn to oxidize test gas [11]. In comparison with single metal oxide gas sensors, the obtained ferrite material sensor elements in some cases are characterized by higher response [22], but in some cases by lower response where SnO_2 nanowires were used [23].

With increasing operating temperature, the response increases to maximum and then decreases (Fig. 6). The maximum response of the sensor element could be attributed to three reasons: (i) increase of the concentration of oxygen species on the surface by replacing adsorbed hydroxyl groups; (ii) conversion of adsorbed oxygen species by the following reactions: $O_{2(gas)} \rightarrow O_{2(ads)} \rightarrow O_{2\ (ads)}^{-} \rightarrow 2O^{-}_{(ads)} \rightarrow 2O^{2-}_{(ads)}$, thus attracting more electrons from the semiconductor and enhancing change in resistivity during the reaction between oxygen and test gas [24]; (iii) increase of the thermal energy of gas molecules to overcome the activation energy barrier of the surface reaction with adsorbed oxygen species [6]; Decrease of the sensitivity after maximum can be attributed to reduction of gas adsorption ability at higher temperatures [6]. Overall maximum response temperature corresponds to the operating sensor temperature and for excess-iron ferrite is situated at 300 °C, but for stoichiometric sample at 275 °C.

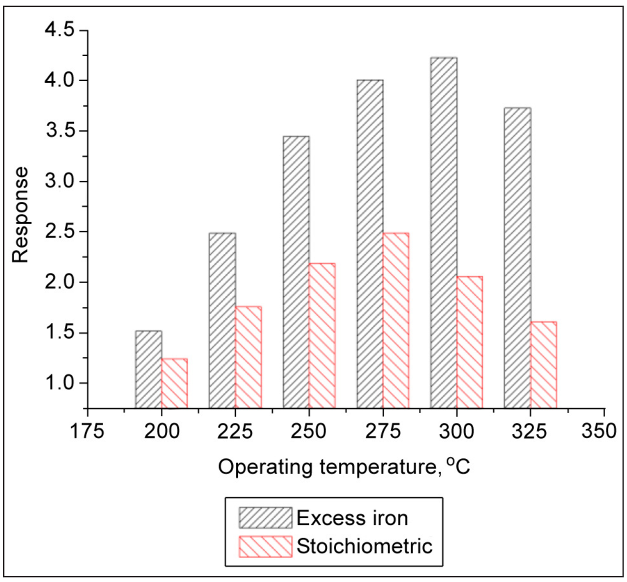

Fig. 6. Response dependence on temperature for stoichiometric and excess-iron Ni-Zn ferrites for the 500 ppm acetone gas

Change of the resistance by gas exposure is shown in Fig. 7. Resistance changes in a moment when gas is introduced into the testing atmosphere. In the same time, the obtained response and recovery time are longer than those of the literature values [18] due to the bulk nature of the sensor element. As we can see, resistance for stoichiometric Ni-Zn ferrite increases, but for excess-iron Ni-Zn ferrite it decreases, attributed to different type of charge carriers.

It is known that electrical resistance for n-type semiconductors decreases, but for p-type it increases when reducing gas reacts with oxygen species absorbed on the grain surface [25]. By interaction with reducing gas, the oxygen

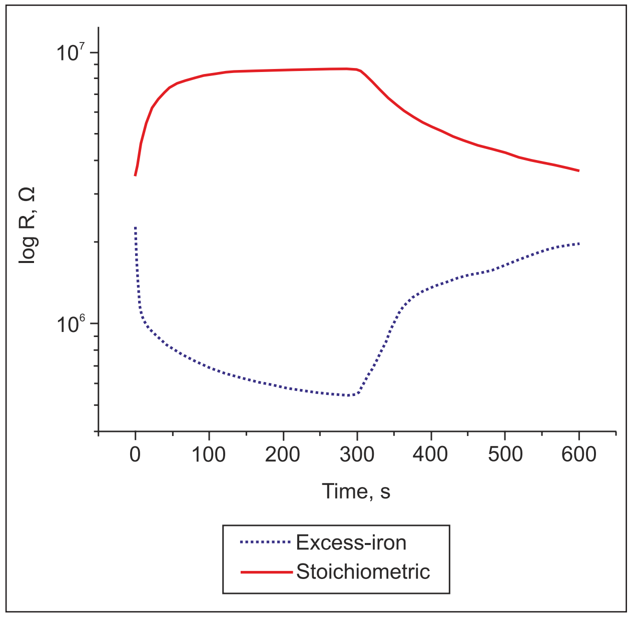

Fig. 7. Conductivity variation with time for stoichiometric and excess-iron Ni-Zn ferrites

concentration on the solid surface decreases thus releasing trapped electrons and introducing them back to the sensor material and decreasing or increasing resistance [24]. Resistance for p-type material increases due to the hole and released electron recombination, thus lowering the charge carrier concentration.

From the observed relationships depicted in Fig. 7 we can conclude that stoichiometric Ni-Zn ferrites possess p-type conductivity, but excess-iron Ni-Zn ferrites possess n-type. This is attributed to the hole transfer between nickel ions in case of $Ni_{0.3}Zn_{0.7}Fe_2O_4$ and the electron transfer between $Ni_{0.3}Zn_{0.7}Fe_{2.1}O_{4-}$ as pointed out in the introduction of the paper. In non-stoichiometric excess-iron ferrites Fe easily dissolves in the spinel phase by partial reduction of Fe from $3Fe_2^{3+}O_3$ to $2Fe^{2+}Fe_2^{3+}O_4$ thus increasing Fe^{2+} concentration and enhancing electron hopping [16].

CONCLUSIONS

As confirmed by the XRD and SEM microanalysis, the sol-gel auto-combustion method can be applied for the synthesis of the nanometric single-phase spinel type Ni-Zn ferrite gas sensor materials with different iron stoichiometry. Stoichiometric Ni-Zn ferrite possesses p-type, but excess-iron ferrite possesses n-type conductivity, giving evidence for Fe^{3+} reduction to Fe^{2+}. Excess-iron Ni-Zn ferrite in comparison with stoichiometric ferrite exhibits higher response to acetone at all tested temperatures, what could be attributed to higher oxygen adsorption ability for interaction with test gas.

ACKNOWLEDGEMENTS

This work was supported by the European Social Fund within the project "Support for the Implementation of Doctoral Studies at Riga Technical University".

Received 14 August 2012
Accepted 21 September 2012

References

1. Sugimoto M. The past, present, and future of ferrites. *Journal of American Ceramic Society.* 1999. Vol. 82. No. 2. P. 269–280.
2. Sutka A., Stingaciu M., Mezinskis G., Lusis A. An alternative method to modify the sensitivity of p-type $NiFe_2O_4$ gas sensor. *Journal of Materials Science.* 2012. Vol. 47. No. 6. P. 2856–2863.
3. Chen N. S., Yang X. J., Liu E. S., Huang J. L. Reducing gas-sensing properties of ferrite compounds MFe_2O_4 (M=Cu, Zn, Cd and Mg). *Sensors and Actuators B: Chemical.* 2000. Vol. 12. No. 1. P. 178–180.
4. Gopal Reddy C. V., Manorama S. V., Rao V. J. Preparation and characterization of ferrites as gas sensor materials. *Journal of Materials Science Letters.* 2000. Vol. 19. No. 9. P. 775–778.
5. Kapse V. D., Ghosh S. A., Raghuwanshib F. C., Kapse S. D., Khandekar U. Nanocrystalline $Ni_{0.6}Zn_{0.4}Fe_2O_4$: A novel semiconductor material for ethanol detection. *Talanta.* 2009. Vol. 78. No. 1. P. 19–25.
6. Kadu A. V., Jagtap S. V., Chaudhari G. N. Studies on the preparation and ethanol gas sensing properties of spinel $Zn_{0.6}Mn_{0.4}Fe_2O_4$ nanomaterials. *Current Applied Physics.* 2009. Vol. 9. No. 6. P. 1246–1251.
7. Mukherjee K., Majumder S. B. Reducing gas sensing behavior of nano-crystalline magnesium-zinc ferrite powders. *Talanta.* 2010. Vol. 81. No. 4–5. P. 1826–1832.
8. Gul I. H., Ahmed W., Maqsood A. Electrical and magnetic characterization of nanocrystalline Ni-Zn ferrite synthesis by co-precipitation route. *Journal of Magnetism and Magnetic Materials.* 2008. Vol. 320. No. 3–4. P. 270–275.
9. Korotcenkov G. The role of morphology and crystallographic structure of metal oxides in response of conductometric-type gas sensors. *Materials Sience and Engineering R: Reports.* 2008. Vol. 61. No. 1–6. P. 1–39.
10. Sutka A., Mezinskis G., Lusis A., Stingaciu M. Gas sensing properties of Zn-doped p-type nickel ferrite. *Sensors and Actuators B: Chemical.* 2012, doi: 10.1016/j.snb.2012.04.059.
11. Sutka A., Mezinskis G., Lusis A., Jakovlevs D. Influence of iron non-stoichiometry on spinel zinc ferrite gas sensing properties. *Sensors and Actuators B: Chemical.* 2012. doi: 10.1016/j.snb.2012.03.012.
12. Varpula A., Novikov S., Haarahiltunen A., Kuivalainen P. Transient characterization techniques for resistive metal oxide gas sensors. *Sensors and Actuators B: Chemical.* 2011. Vol. 159. No. 1. P. 12–26.
13. Shobana M. K., Rajendran V., Jeyasubramanian K., Kumar N. S. Preparation and characterisation of NiCo ferrite nanoparticles. *Materials Letters.* 2007. Vol. 61. No. 13. P. 2616–2619.
14. Tianshu Z., Hing P., Jiancheng Z., Lingbing K. Ethanol-sensing characteristics of cadmium ferrite prepared by chemical coprecipitation. *Materials Chemistry and Physics.* 1999. Vol. 61. No. 3. P. 192–198.
15. McCafferty E., Zettlemoyer A. C. Adsorption of water vapour on α-Fe_2O_3. *Discussions on Faraday Society.* 1971. Vol. 52. P. 239–254.
16. Arshak K., Gaidan I. NiO/Fe_2O_3 polymer thick films as room temperature gas sensors. *Thin Solid Films.* 2006. Vol. 495. No. 1–2. P. 286–291.
17. Korotcenkov G. Metal oxides for solid-state gas sensors: What determines our choice? *Material Science and Engineering B.* 2007. Vol. 139. No. 1. P. 1–23.
18. Tiemann M. Porous metal oxides as gas sensors. *Chemistry – A European Journal.* 2007. Vol. 13. No. 30. P. 8376–8388.
19. Valenzuela R. *Magnetic Ceramics*. Melbourne: Cambridge University Press, 1994. 181 p.
20. Kotnala R. K., Shah J., Singh B., Kishan H., Singh S., Dhawan S. K., Sengupta A. Humidity response of Li-substituted magnesium ferrite. *Sensors and Actuators B: Chemical.* 2008. Vol. 129. No. 2. P. 909–914.
21. Caldararu M., Sprinceana D., Popa V. T., Ionescu N. I. Surface dynamics in tin dioxide-containing catalysts II. Competition between water and oxygen adsorption on polycrystalline tin dioxide sensor. *Sensors and Actuators B: Chemical.* 1996. Vol. 30. No. 1. P. 35–41.
22. Li X., Chang Y., Long Y. Influence of Sn doping on ZnO sensing properties for ethanol and acetone. *Material Science and Engineering C.* 2012. Vol. 32. No. 4. P. 817–821.
23. Qin L., Xu J., Dong X., Pan Q., Cheng Z., Xiang Q., Li F. The template-free synthesis of square-shaped SnO_2 nanowires: the temperature effect and acetone gas sensors. *Nanotechnology.* 2008. Vol. 19. No. 18. 185705 (8 pages).
24. Moseley P. T. New trends and future prospects of thick- and thin-film gas sensors. *Sensors and Actuators B: Chemical.* 1991. Vol. 3. No. 3. P. 164–174.
25. Arshak K., Gaidan I. Development of a novel gas sensor based on oxide thick films. *Materials Science and Engineering B.* 2005. Vol. 118. No. 1–3. P. 44–49.

Andris Sutka, Gundars Mezinskis, Gundars Strikis, Andreis Siskin

DUJŲ JAUTRUMAS STECHIOMETRINIAM IR GELEŽIES PERTEKLIŲ TURINČIAM Ni-Zn FERITUI, PAGAMINTAM *SOL-GEL* METODU AUTONOMINIAME DEGIMO PROCESE

Santrauka

Darbo tikslas – palyginti dujų reakciją į nanostruktūrizuoto autodegimo būdu gauto stechiometrinio ir geležimi prisotinto nikelio-cinko ferito ($Ni_{0.3}Zn_{0.7}Fe_{2+z}O_4$, kur z = 0 ir 0,1) acetoną. Darbe išsamiai analizuojami sintezės etapai ir dujų jautrumo matavimo metodologija. Jutiklio medžiaga buvo ištirta rentgeno spindulių difrakcinės analizės metodu skenuojant elektronų mikroskopu (SEM) bei pastoviosios srovės (DC) atsparumo skaičiavimais. Rentgeno spindulių difrakcinės analizės metodas patvirtina, kad mėginiai suformavo vienafazę struktūrą, SEM nustatytos mažesnės nei 100 nm nanogranulės. Atsparumo laukai, palyginti su temperatūra, lemia adsorbuoto vandens poveikį laidumui. Turėdamas geležies perteklių, Ni-Zn feritas keičia savo DC elektros atsparumą, laidumo tipą ir reakciją dujų mažėjimui (daugiau nei 2 kartus). Gautąsias priklausomybes galima paaiškinti Fe susidarymu medžiagoje bei padidėjusia elektrinio krūvio nešėjų (elektronų) koncentracija. Tai iššaukia deguonies adsorbcijos gebą, kuri gali reaguoti su bandomosiomis dujomis.

Raktažodžiai: nikelio-cinko feritas, (ne)stechiometrija, dujų jutiklis, degimo sintezė

Андрис Сутка, Гундарс Мезинский, Гундарс Стрикис, Андрейс Сискин

ЧУВСТВИТЕЛЬНОСТЬ ГАЗОВ СТЕХИОМЕТРИЧЕСКОМУ, С ИЗЛИШКОМ ЖЕЛЕЗА ФЕРРИТУ Ni-Zn, СИНТЕЗИРОВАННОМУ *SOL-GEL* МЕТОДОМ В ПРОЦЕССЕ АУТО-ГОРЕНИЯ

Резюме

Применение новых материалов предоставляет возможность использовать более чувствительные, селективные и стабильные, долгосрочные материалы для создания датчиков. Цель данного исследования – сопоставить реакции газов в нано структурные соединения, полученных методом ауто-горения стехиометрического и железом насыщенного никель-цинк феррита ($Ni_{0,3}Zn_{0,7}Fe_{2+z}O_4$, где z = 0 и 0,1).

В работе представлены этапы синтеза и методология измерения чувствительности газов. Материалы датчиков исследованы методом дифракционного анализа рентгеновских лучей сканирующего электронного микроскопа и расчетами сопротивления на основе измеренения постоянного тока. Метод дифракционного анализа рентгеновских лучей подтверждает, что в опытах была сформирована однофазная структура. Сканирующим электронным микроскопом были определены нано-гранулы диаметром меньше 100 nm. Поля устойчивости по сравнению с температурой показывают влияние адсорбированной воды на проводимость. Из-за большого количества железа Ni-Zn феррит изменяет своё электрическое сопротивление, тип проводимости и реакцию уменьшения газов (больше чем 2 раза). Полученные зависимости обусловлены образованием железа (Fe) в материале, что увеличивает концентрацию электронов и способность абсорбирования кислорода реагирующего с исследуемыми газами.

Ключевые слова: Ni-Zn феррит, нестехиометрия, газовый датчик, синтез горения